Alexandria Engineering Journal (2016) 55, 1085–1098

HOSTED BY ELSEVIER

Alexandria University

Alexandria Engineering Journal

www.elsevier.com/locate/aej
www.sciencedirect.com

ORIGINAL ARTICLE

Analytical solution for peristaltic flow of conducting nanofluids in an asymmetric channel with slip effect of velocity, temperature and concentration

S. Sreenadh [a], A.N.S. Srinivas [b,*], C.K. Selvi [b]

[a] Department of Mathematics, Sri Venkateswara University, Tirupati, India
[b] School of Advanced Sciences, VIT University, Vellore, Tamil Nadu, India

Received 12 January 2016; revised 26 February 2016; accepted 15 March 2016
Available online 8 April 2016

KEYWORDS

Peristaltic transport;
Nanofluids;
Magnetic effect;
Slip parameter;
Asymmetric channel

Abstract The Peristaltic transport of conducting nanofluids under the effect of slip condition in an asymmetric channel is reported in the present work. The mathematical modelling has been carried out under long wavelength and low Reynolds number approximations. The analytical solutions are obtained for pressure rise, nanoparticle concentration, temperature distribution, velocity profiles and stream function. Influence of various parameters on the flow characteristics has been discussed with the help of graphs. The results showed that the pressure rise increases with increasing magnetic effect and decreases with increasing slip parameter. The effects of thermophoresis parameter and Brownian motion parameter on the nanoparticle concentration and temperature distribution are studied. It is observed that the pressure gradient increases with increasing slip parameter and magnetic effect. The trapping phenomenon for different parameters is presented.

1. Introduction

In recent times, Peristalsis has attracted much attention due to its important in engineering and medical applications such as chyme movement in the intestine, movement of ovum in the fallopian tube, flow from kidney to bladder, capillaries, arterioles and roller pumps. In view of such industrial and physiological applications, the peristalsis mechanism has been studied in nature by various researchers for different fluids under different conditions [1–8]. Nanoparticle research is currently an area of intense scientific interest due to a wide variety of potential applications in medical and electronic field. The nanofluids are a new class of fluids designed by dispersing nano-meter sized materials (nanoparticles, nanofibers, nanotubes, nanorods, nanosheet and nanowires) in base fluids. Choi and Eastman [9] was reported that an innovative technique to improve heat transfer is by using nanoscale particles in base fluid. In the other work by Choi et al. [10] it was also shown that the addition of small amount (less than 1% by volume) of nanoparticles to conventional heat transfer liquids increases the thermal conductivity of the fluid approximately two times.

* Corresponding author. Mobile: +91 8903312379.
E-mail address: anssrinivas@vit.ac.in (A.N.S. Srinivas).
Peer review under responsibility of Faculty of Engineering, Alexandria University.

http://dx.doi.org/10.1016/j.aej.2016.03.015
1110-0168 © 2016 Faculty of Engineering, Alexandria University. Production and hosting by Elsevier B.V.

Nomenclature

$a_1,\ b_1$	amplitudes of the waves	θ	temperature distribution
$d_1 + d_2$	channel width	β	the slip parameter
λ	wavelength of the peristaltic wave	γ	thermal slip parameter
c	wave speed	γ_1	concentration slip parameter
p	pressure	N_t	Brownian motion parameter
ϕ	phase difference	N_b	thermophoresis parameter
μ	viscosity	G_r	local temperature Grashof number
M	Hartmann number	B_r	nanoparticle Grashof number
B_0	uniform magnetic field	σ	nanoparticle concentration
ψ	steam function		

A detailed analysis of nanofluids was discussed by Buongiorno [11] reveals that this massive increase in the thermal conductivity occurs due to the presence of two main effects namely the Brownian diffusion and thermophoretic diffusion of nanoparticles. Mekheimer and Abd elmaboud [12] pointed out that the cancer tissues may be destroyed when the temperature reaches 40–45 °C. The influence of slip conditions, wall properties and heat transfer on MHD peristaltic transport was studied by Srinivas et al. [13]. Peristaltic transport of a Jeffrey fluid under the effect of slip in an inclined asymmetric channel was studied by Srinivas and Muthuraj [14]. Endoscopic effects on peristaltic flow of nanofluids are studied by Akbar and Nadeem [15]. Ramana Kumari and Radhakrishnamacharya [16] have investigated effect of slip on heat transfer to peristaltic transport in the presence of magnetic field with wall effects. Further the study of Peristaltic flow of a nanofluid in non-uniform tube is done by Akbar et al. [17] using Homotopy Perturbation method. Akbar and Nadeem [18] have investigated the peristaltic flow of a Phan-Thien–Tanner nanofluid in a diverging tube. The analytical and numerical solutions for influence of wall properties on the peristaltic flow of a nanofluid were studied by Mustafa et al. [19]. Further Akbar et al. [20] have studied peristaltic flow of a nanofluid with slip effects. A note on the influence of heat and mass transfer on a peristaltic flow of a viscous fluid in a vertical asymmetric channel with wall slip was studied by Srinivas et al. [21].

Akram et al. [22] have studied consequences of nanofluids on peristaltic flow in an asymmetric channel. Numerical study of Williamson nanofluid in an asymmetric channel is investigated by Akbar et al. [23]. Exact analytical solution of the peristaltic nanofluids flow in an asymmetric channel with flexible walls and slip condition: Application to cancer treatment was discussed by Ebaid et al. [24]. Slip effects on the Peristaltic motion of nanofluids in a channel with wall properties were studied by Mustafa et al. [25].

Recently exact analytical solution for the peristaltic flow of nanofluids in an asymmetric channel with slip effect of the velocity, temperature and concentration was studied by Aly et al. [26]. The study on consequence of nanofluids on peristaltic transport of a hyperbolic tangent fluid model in the occurrence of apt (tending) magnetic field was discussed by Akram and Nadeem [27].

Mustafa et al. [28] studied the influence of induced magnetic field on the peristaltic flow of nanofluids. Peristaltic motion of nanofluids in curved channel was analysed by Hina et al. [29]. Sharidan Shafie et al. [30] studied Partial slip effect on heat and mass transfer of MHD peristaltic transport in a porous medium. Hayat et al. [31] studied Peristaltic transport of Carreau-Yasuda fluid in a curved channel with slip effects.

The nanofluids in peristaltic flow problem under the effect of magnetic field and radiation in the tapered asymmetric channel through porus space was described by Kothandapani and Prakash [32]. The peristaltic transport of Carreau nanofluids under the effect of magnetic field in a tapered asymmetric channel was studied by Kothandapani and Prakash [33]. Effect of thermal radiation parameter and magnetic field on the peristaltic motion of Williamson nanofluids in a tapered asymmetric channel was studied by Kothandapani and Prakash [34]. Nirmala et al. [35] studied combined effects of hall current, wall slip, viscous dissipation and soret effect on MHD Jeffrey fluid flow in a vertical channel with Peristalsis.

The Present work was to discuss the peristaltic flow of nanofluids in an asymmetric channel under the effect of both magnetic field and slip parameters. The governing equations are carried out under the assumption of long wavelength and low Reynolds number. The reduced equations are solved exactly.

The result of the present study finds applications in peristaltic pumping through corrogative and non-corrogative pipes. In the case of corrogative pipe flow the slip effect is important, whereas in the other case slip may not exist.

2. The mathematical model

Consider peristaltic transport of an incompressible Newtonian conducting nanofluid in an asymmetric channel with flexible walls. The channel asymmetry is generated by propagation of waves on the channel walls travelling with different amplitudes and phases but with same constant speed c.

In the Cartesian coordinates system $(\bar{X}, \bar{Y})$ of the fixed frame, the upper wall $\bar{h}_1$ and lower wall $\bar{h}_2$ are given by Fig. 1

$$\left\{ \begin{array}{l} \bar{h}_1 = d_1 + a_1 \cos\left(\frac{2\pi}{\lambda}\left[\bar{X} - c\bar{t}\right]\right), \\ \bar{h}_2 = -d_2 - b_1 \cos\left(\frac{2\pi}{\lambda}\left[\bar{X} - c\bar{t}\right] + \varphi\right) \end{array} \right\}$$

where a_1 and b_1 are amplitude of the waves, λ is the wavelength, $d_1 + d_2$ is the width of the channel, and the phase difference ϕ varies in the range $0 \leqslant \phi \leqslant \pi$ where $\phi = 0$ and $\phi = \pi$ correspond to symmetric cannel with waves out of the

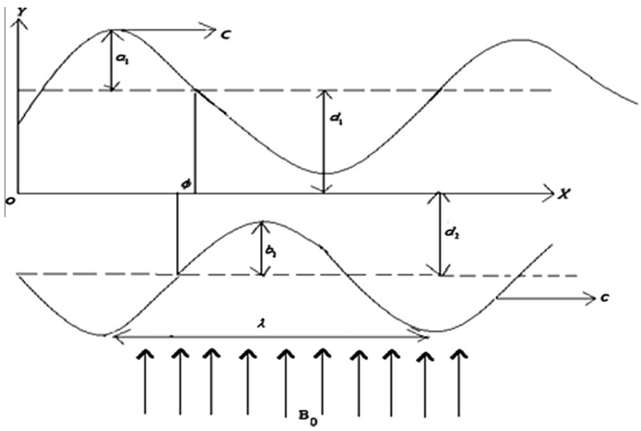

Figure 1 Physical model.

phase and in the phase, respectively. Further, a_1, b_1, d_1, d_2 and ϕ satisfy the following condition [32].

$$a_1^2 + b_1^2 + 2a_1 b_1 \cos\varphi \leqslant (d_1 + d_2)^2$$

With the following non-dimensional phenomena

$$a = \frac{a_1}{d_1}, b = \frac{a_2}{d_1}, d = \frac{d_2}{d_1}$$

In the moving frame of reference $(\overline{X}, \overline{Y})$, we have

$$\bar{x} = \overline{X} - c\bar{t}, \bar{y} = \overline{Y}$$

The non-dimensional quantities are

$$x = \frac{2\pi\bar{x}}{\lambda}, \quad y = \frac{\overline{Y}}{d_1}, \quad t = \frac{2\pi\bar{t}}{\lambda}, \quad h_1 = \frac{\bar{h}_1}{d_1}, \quad h_2 = \frac{\bar{h}_2}{d_2}, M = \sqrt{\frac{\sigma}{\mu}} dB_0$$

Under the assumptions of long wavelength and low Reynolds number approximation, Kothandapani and Prakash [32] found that the flow is governed by the following system of partial differential equations in non-dimensional form

$$\frac{\partial^2}{\partial y^2}\left[\frac{\partial^2\psi}{\partial y^2} - M^2\psi\right] + G_r\frac{\partial\theta}{\partial y} + B_r\frac{\partial\sigma}{\partial y} = 0 \quad (1)$$

$$\frac{dp}{dx} = \frac{\partial}{\partial y}\left[\frac{\partial^2\psi}{\partial y^2} - M^2\psi\right] + G_r\theta + B_r\sigma \quad (2)$$

$$\frac{\partial^2\theta}{\partial y^2} + N_b\frac{\partial\theta}{\partial y}\frac{\partial\sigma}{\partial y} + N_t\left(\frac{\partial\theta}{\partial y}\right)^2 = 0 \quad (3)$$

$$\frac{\partial^2\sigma}{\partial y^2} + \frac{N_t}{N_b}\left(\frac{\partial^2\theta}{\partial y^2}\right) = 0 \quad (4)$$

where ψ, θ, σ and P are the stream function, temperature distribution, nanoparticle concentration and pressure gradient respectively. Further N_t, N_b, G_r, B_r and M are Brownian motion parameter, thermophoresis parameter, local temperature Grashof number, nanoparticle Grashof number and Hartmann number respectively.

The corresponding boundary conditions are

$$\psi = \frac{F}{2}, \frac{\partial\psi}{\partial y} = -\beta\frac{\partial^2\psi}{\partial y^2} - 1 \text{ at } h_1 = 1 + a\cos(x) \quad (5)$$

$$\psi = -\frac{F}{2}, \frac{\partial\psi}{\partial y} = \beta\frac{\partial^2\psi}{\partial y^2} - 1 \text{ at } h_2 = -d - b\cos(x + \varphi) \quad (6)$$

$$\theta + \gamma\frac{\partial\theta}{\partial y} = 0 \text{ at } y = h_1 \quad (7)$$

$$\theta - \gamma\frac{\partial\theta}{\partial y} = 1 \text{ at } y = h_2 \quad (8)$$

$$\sigma + \gamma_1\frac{\partial\sigma}{\partial y} = 0 \text{ at } y = h_1 \quad (9)$$

$$\sigma - \gamma_1\frac{\partial\sigma}{\partial y} = 1 \text{ at } y = h_2 \quad (10)$$

where β, γ and γ_1 represent the slip parameter, thermal slip parameter and concentration slip parameter respectively.

3. The general closed form solution

Now from Eq. (4) we obtain,

$$\sigma = -\frac{N_t}{N_b}\theta + c_1(x)y + c_2(x) \quad (11)$$

where $c_1(x)$ and $c_2(x)$ are two unknown functions. By substituting Eq. (11) into (3) gives

$$\frac{\partial^2\theta}{\partial y^2} + N_b c_1(x)\frac{\partial\theta}{\partial y} = 0 \quad (12)$$

The above equation can be solved exactly to get the temperature distribution as

$$\theta(x, y) = c_4(x)e^{-N_b f_1(x)y} + \frac{1}{N_b}\frac{c_3(x)}{c_1(x)} \quad (13)$$

The nanoparticle concentration is given by

$$\sigma(x, y) = -\frac{N_t}{N_b}c_4(x)e^{-N_b c_1(x)y} + c_1(x)y + c_2(x) - \frac{N_t}{N_b^2}\frac{c_3(x)}{c_1(x)} \quad (14)$$

where $c_3(x)$ and $c_4(x)$ are two unknown functions. By substituting boundary conditions (7) and (8) in Eq. (13) gives

$$c_4(x)e^{-N_b c_1(x)h_1}[1 - \gamma N_b c_1] = -\frac{1}{N_b}\frac{c_3(x)}{c_1(x)} \quad (15)$$

$$c_4(x)e^{-N_b c_1(x)h_2}[1 + \gamma N_b c_1] = 1 - \frac{1}{N_b}\frac{c_3(x)}{c_1(x)} \quad (16)$$

By solving Eqs. (15) and (16) for $c_3(x)$ and $c_4(x)$ we have

$$c_4 = \frac{1}{(1 + \gamma N_b c_1)r_2^{c_1} - (1 - \gamma N_b c_1)r_1^{c_1}} \quad (17)$$

and

$$c_3 = \frac{-N_b c_1(1 - \gamma N_b c_1)r_1^{c_1}}{(1 + \gamma N_b c_1)r_2^{c_1} - (1 - \gamma N_b c_1)r_1^{c_1}} \quad (18)$$

Where $r_1 = e^{-N_b h_1}$ and $r_2 = e^{-N_b h_2}$ (19)

Applying boundary conditions (9) and (10) in Eq. (14) gives

$$\left(\gamma_1 c_1 - \frac{1}{N_b}\right)N_t c_4 r_1^{c_1} + (\gamma_1 + h_1)c_1 + \left(c_2 - \frac{N_t}{N_b^2}\frac{c_3}{c_1}\right) = 0 \quad (20)$$

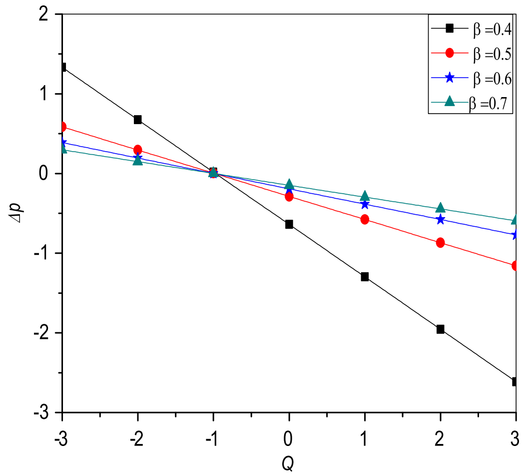

(a) $a=0.3, b=0.5, N_t=0.5, N_b=0.8, d=1, \phi=0.3,$
$\gamma=0.5, \gamma_1=0.5, M=3, B_r=0.5, G_r=0.5$

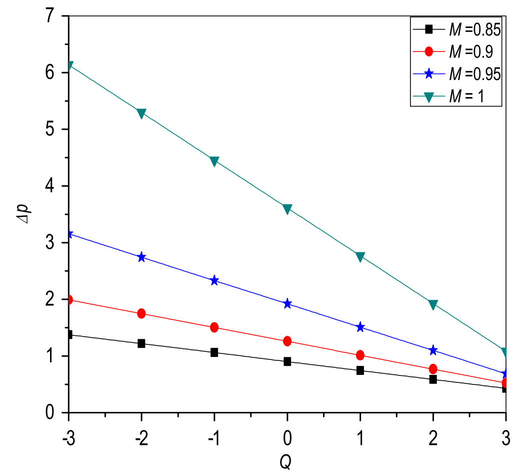

(b) $a=0.2, b=0.3, N_t=2, N_b=0.8, d=1,$
$\phi=0.3, \gamma=0.5, \gamma_1=0.5, \beta=0.1, B_r=0.5, G_r=0.5$

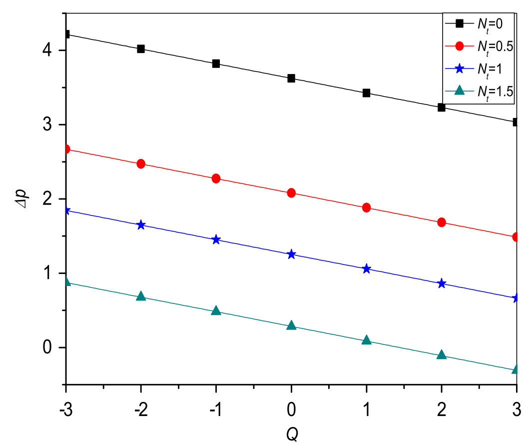

(c) $a=0.6, b=0.5, M=0.8, N_b=0.5, d=1,$
$\phi=0.3, \gamma=0.5, \gamma_1=0.5, \beta=0.3, B_r=1.5, G_r=1.3$

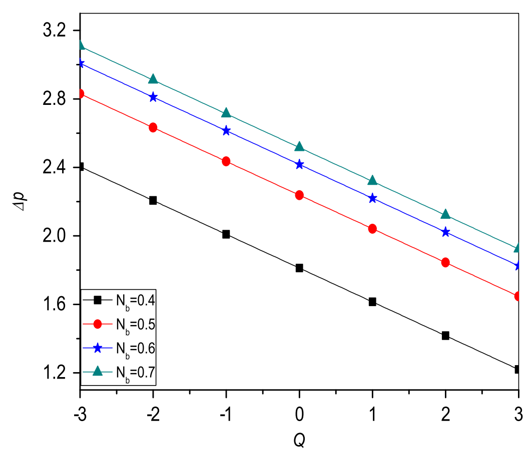

(d) $a=0.6, b=0.5, M=0.8, N_t=0.5, d=1,$
$\phi=0.3, \gamma=0.5, \gamma_1=0.5, \beta=0.3, B_r=1.5, G_r=1.3$

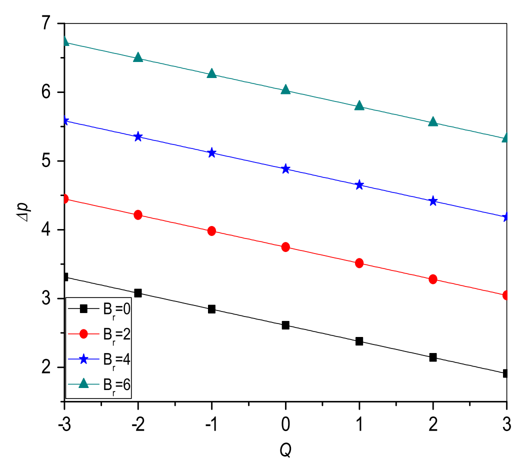

(e) $a=0.4, b=0.5, N_t=2, N_b=3, d=1, \phi=0.3,$
$\gamma=0.5, \gamma_1=0.5, M=0.8, \beta=0.3, G_r=2$

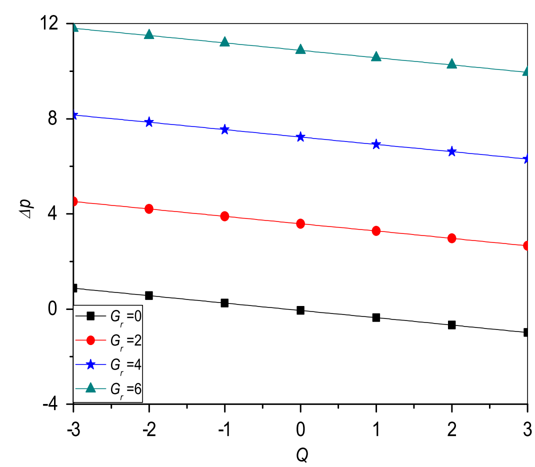

(f) $a=0.4, b=0.3, N_t=1, N_b=0.5, d=1, \phi=0.3,$
$\gamma=0.5, \gamma_1=0.5, M=0.8, \beta=0.3, B_r=1$

Figure 2 Variation of pressure rise versus flow rate.

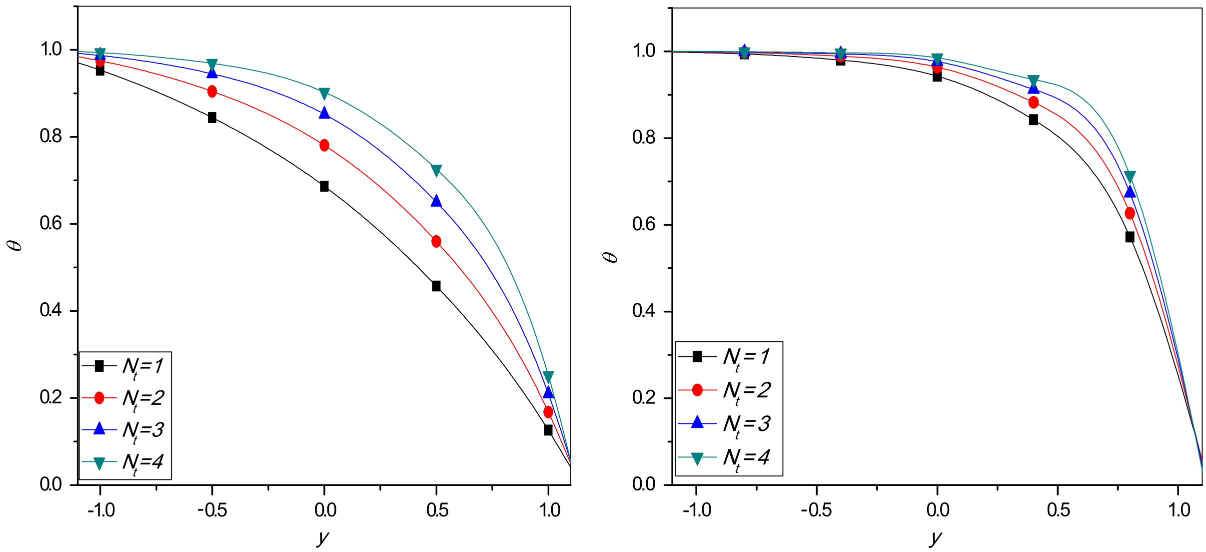

(a) $a = 0.1, b = 0.5, d = 1, \phi = 0.2, \gamma = 0.1, \gamma_1 = 0.1, x = 1, N_b = 0.8$

(b) $a = 0.1, b = 0.5, d = 1, \phi = 0.2, \gamma = 0.1, \gamma_1 = 0.1, x = 1, N_b = 5$

Figure 3 Variation of temperature profile θ for different values of N_t.

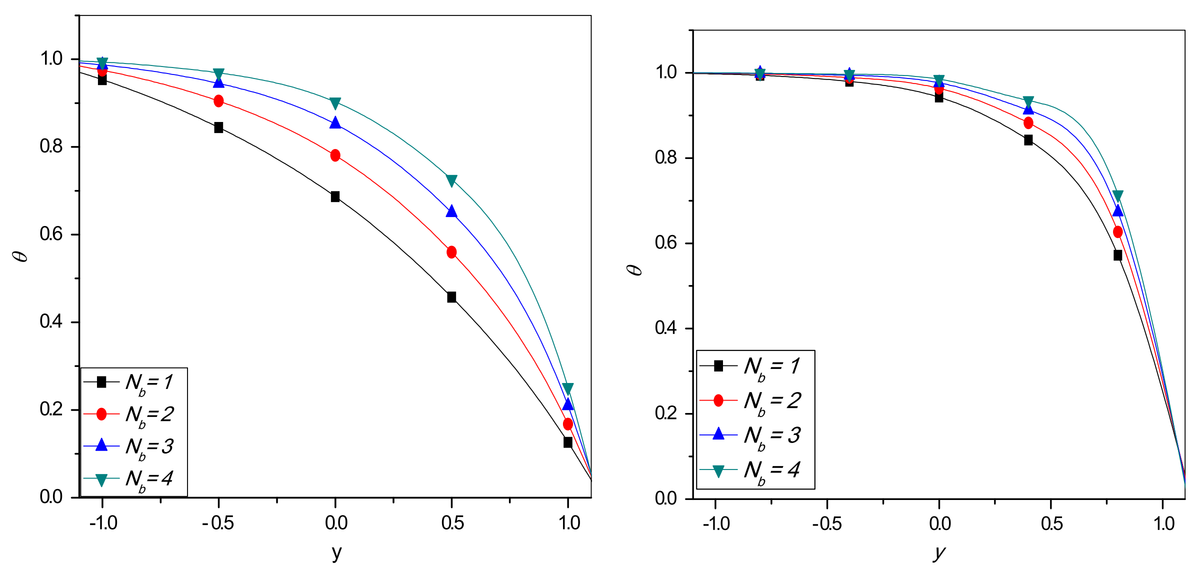

(a) $a = 0.1, b = 0.5, d = 1, \phi = 0.2, \gamma = 0.1, \gamma_1 = 0.1, x = 1, N_t = 0.8$

(b) $a = 0.1, b = 0.5, d = 1, \phi = 0.2, \gamma = 0.1, \gamma_1 = 0.1, x = 1, N_t = 5$

Figure 4 Variation of temperature profile θ for different values of N_b.

$$\left(\gamma_1 c_1 + \frac{1}{N_b}\right) N_t c_4 r_2^{c_1} + (\gamma_1 - h_2)c_1 - \left(c_2 - \frac{N_t}{N_b^2}\frac{c_3}{c_1}\right) = -1 \tag{21}$$

Therefore $c_2(x)$ is given from Eq. (20) is

$$c_2 = \frac{N_t}{N_b^2}\frac{c_3}{c_1} - \left(\gamma_1 c_1 - \frac{1}{N_b}\right) N_t c_4 r_1^{c_1} - (\gamma_1 + h_1)c_1 \tag{22}$$

By eliminating $c_2(x)$ from Eqs. (22) and (23) to obtain we get,

$$N_t c_4\left[\left(\gamma_1 c_1 - \frac{1}{N_b}\right) r_1^{c_1} + \left(\gamma_1 c_1 + \frac{1}{N_b}\right) r_2^{c_1}\right] + (2\gamma_1 + h_1 - h_2)c_1 = -1 \tag{23}$$

This can be written as

$$\frac{N_t}{N_b}\left[\frac{(\gamma_1 N_b c_1 - 1) r_1^{c_1} + (\gamma_1 N_b c_1 + 1) r_2^{c_1}}{(\gamma N_b c_1 - 1) r_1^{c_1} + (\gamma N_b c_1 + 1) r_2^{c_1}}\right] + (2\gamma_1 + h_1 - h_2)c_1 = -1 \tag{24}$$

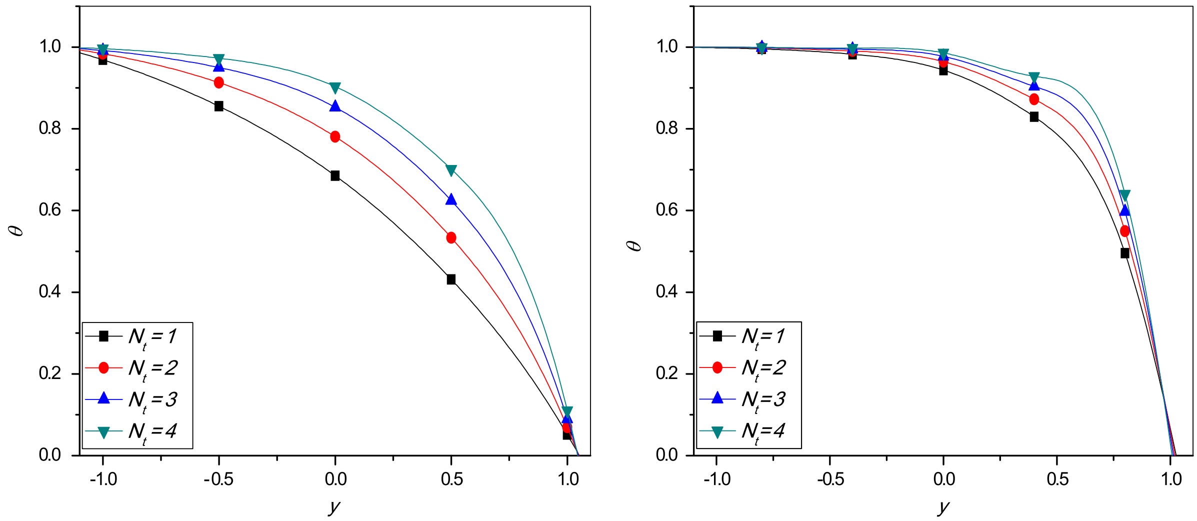

(a) $a = 0.1, b = 0.5, d = 1, \phi = 0.2,$
$\gamma = \gamma_1 = 0, x = 1, N_b = 0.8$

(b) $a = 0.1, b = 0.5, d = 1, \phi = 0.2,$
$\gamma = \gamma_1 = 0, x = 1, N_b = 5$

Figure 5 Temperature distribution θ for different values of N_t (without slip parameters).

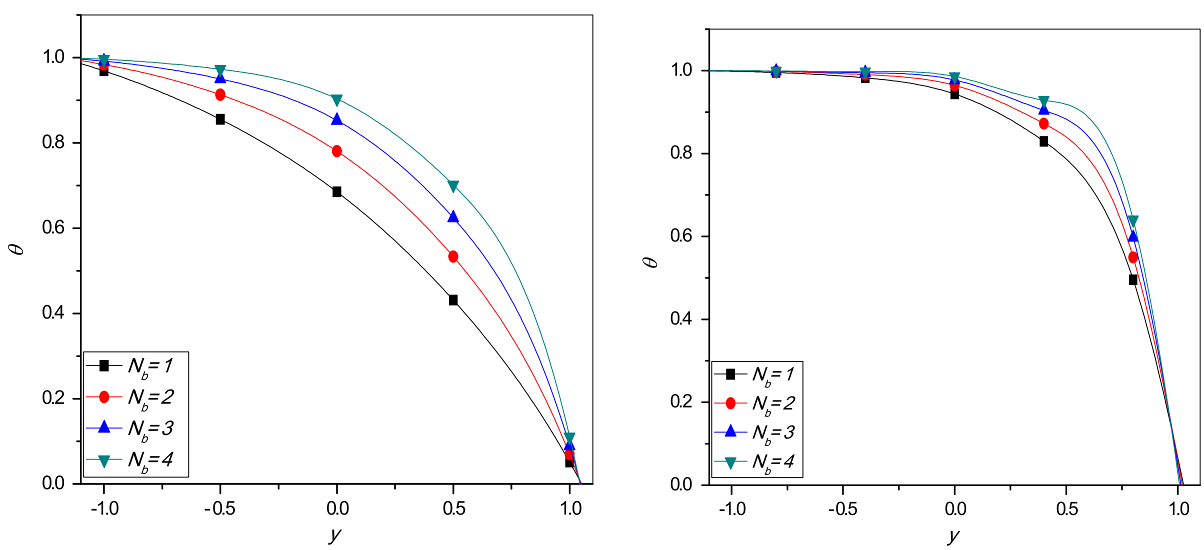

(a) $a = 0.1, b = 0.5, d = 1, \phi = 0.2,$
$\gamma = \gamma_1 = 0, x = 1, N_t = 0.8$

(b) $a = 0.1, b = 0.5, d = 1, \phi = 0.2,$
$\gamma = \gamma_1 = 0, x = 1, N_t = 5$

Figure 6 Variation of temperature profile θ for different values of N_b (without slip parameter).

which leads to an implicit algebraic equation in $c_1(x)$ and exact solution is difficult to obtain; however, such exact solution is possible when $\gamma = \gamma_1$.

Substituting $\gamma = \gamma_1$ in Eq. (24), we obtain the exact value of $c_1(x)$

$$c_1(x) = \frac{1 + \frac{N_t}{N_b}}{h_2 - h_1 - 2\gamma_1} \tag{24a}$$

Therefore,

$$\left\{ \begin{array}{l} c_2 = \frac{N_t}{N_b^2}\frac{c_3}{c_1} - \left(\gamma_1 c_1 - \frac{1}{N_b}\right) N_t c_4 r_1^{c_1} - (\gamma_1 + h_1) c_1 \\ c_3 = \frac{-N_b c_1 (1 - \gamma N_b c_1) r_1^{c_1}}{(1 + \gamma N_b c_1) r_2^{c_1} - (1 - \gamma N_b c_1) r_1^{c_1}} \\ c_4 = \frac{1}{(1 + \gamma N_b c_1) r_2^{c_1} - (1 - \gamma N_b c_1) r_1^{c_1}} \end{array} \right\} \tag{24b}$$

To obtain the stream function $\psi(x, y)$, Consider Eq. (1)

$$\frac{\partial}{\partial y}\left[\frac{\partial^2\psi}{\partial y^2} - M^2\psi\right] = -G_r\theta - B_r\sigma + c_5 \tag{25}$$

$$= \Omega_1(x) + \Omega_2(x)e^{-N_b c_1 y} - B_r c_1 y + c_5 \tag{26}$$

Where

$$\left\{\begin{array}{l} \Omega_1(x) = \left(\frac{B_r N_t}{N_b} - G_r\right)\frac{1}{N_b}\frac{c_3}{c_1} - B_r c_2 \\ \Omega_2(x) = \left(\frac{B_r N_t}{N_b} - G_r\right)c_4 \end{array}\right\} \tag{27}$$

Now the stream function is given by

$$\psi(x,y) = c_8 e^{My} + c_7 e^{-My} - \frac{1}{M^2}c_6 - \frac{1}{M^2}c_5 y + g(y) \tag{28}$$

Where

$$g(y) = -\frac{1}{M^2}\Omega_1 y - \frac{1}{N_b c_1\left(N_b^2 c_1^2 - M^2\right)}\Omega_2 e^{-N_b c_1 y} + \frac{B_r c_1}{2M^2}\left(y^2 + \frac{2}{M^2}\right) \tag{29}$$

Applying the boundary conditions (5) and (6) in Eqs. (28) and (29),

We obtain the following system of equations

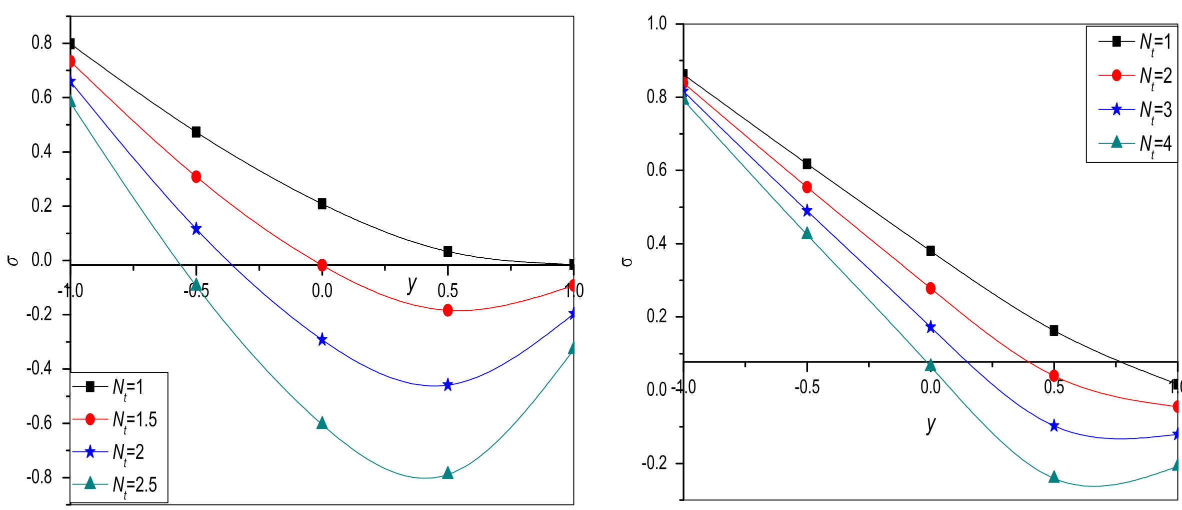

(a) $a = 0.1, b = 0.5, d = 1, \phi = 0.2, \gamma = 0.1, \gamma_1 = 0.1, x = 1, N_b = 0.8$ **(b)** $a = 0.1, b = 0.5, d = 1, \phi = 0.2, \gamma = 0.1, \gamma_1 = 0.1, x = 1, N_b = 5$

Figure 7 Variation of nanoparticle profile σ at different values of N_t.

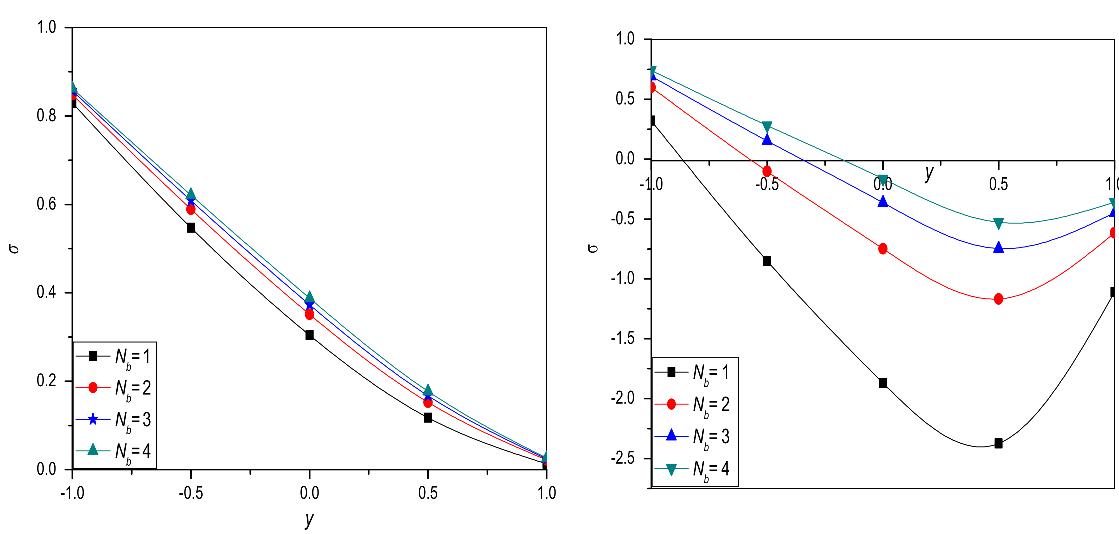

(a) $a = 0.1, b = 0.5, d = 1, \phi = 0.2, \gamma = 0.1, \gamma_1 = 0.1, x = 1, N_t = 0.8$ **(b)** $a = 0.1, b = 0.5, d = 1, \phi = 0.2, \gamma = 0.1, \gamma_1 = 0.1, x = 1, N_t = 5$

Figure 8 Variation of nanoparticle profile σ at different values of N_b.

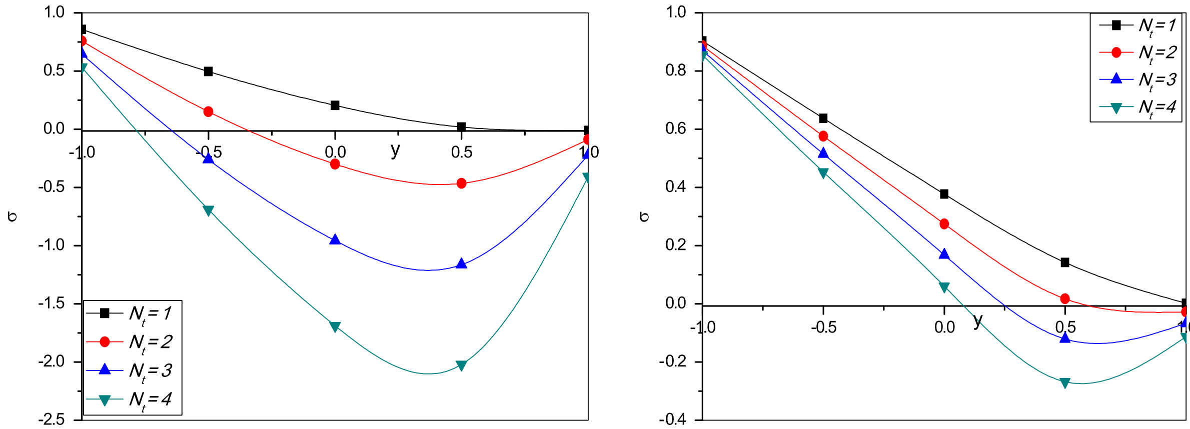

(a) $a = 0.1, b = 0.5, d = 1, \phi = 0.2,$
$\gamma = \gamma_1 = 0, x = 1, N_b = 0.8$

(b) $a = 0.1, b = 0.5, d = 1, \phi = 0.2,$
$\gamma = \gamma_1 = 0, x = 1, N_b = 5$

Figure 9 Variation of nanoparticle profile σ at different values of N_t (without slip parameter).

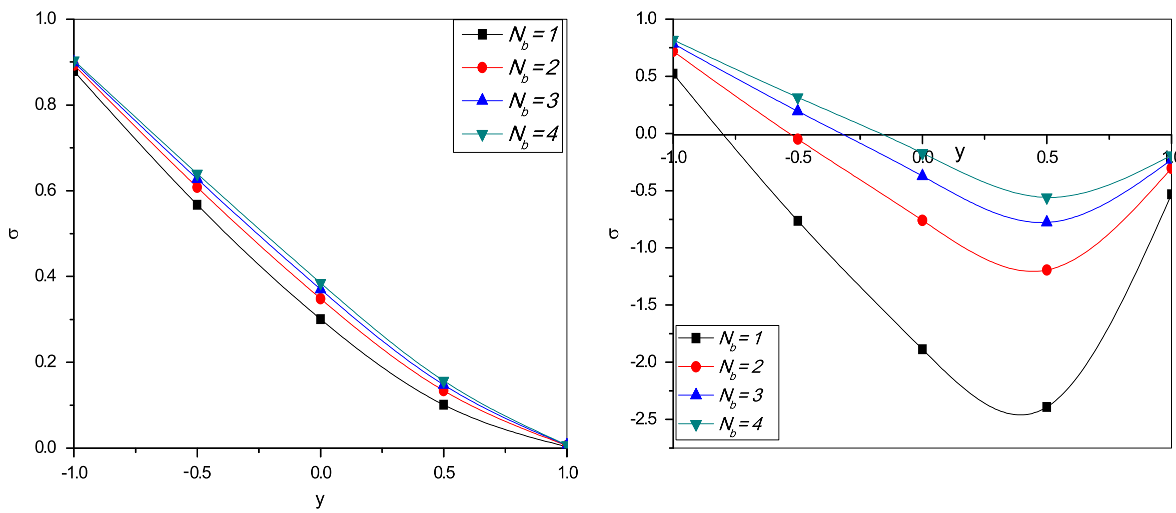

(a) $a = 0.1, b = 0.5, d = 1, \phi = 0.2,$
$\gamma = \gamma_1 = 0, x = 1, N_t = 0.8$

(b) $a = 0.1, b = 0.5, d = 1, \phi = 0.2,$
$\gamma = \gamma_1 = 0, x = 1, N_t = 5$

Figure 10 Variation of nanoparticle profile σ at different values of N_b (without slip parameter).

$$c_8 e^{Mh_1} + c_7 e^{-Mh_1} - c_6 \frac{1}{M^2} - c_5 \frac{h_1}{M^2} = R_1(x)$$
$$c_8 e^{Mh_2} + c_7 e^{-Mh_2} - c_6 \frac{1}{M^2} - c_5 \frac{h_2}{M^2} = R_2(x)$$
$$c_8 e^{Mh_1}(M + M^2\beta) + c_7 e^{-Mh_1}(-M + M^2\beta) - c_5 \frac{1}{M^2} = S_1(x)$$
$$c_8 e^{Mh_2}(M - M^2\beta) + c_7 e^{-Mh_2}(-M - M^2\beta) - c_5 \frac{1}{M^2} = S_2(x) \quad (30)$$

Where

$$R_1(x) = \frac{F}{2} - g(h_1)$$
$$R_2(x) = -\frac{F}{2} - g(h_2) \quad (31)$$
$$S_1(x) = -1 - g'(h_1) - \beta g''(h_1)$$
$$S_2(x) = -1 - g'(h_2) + \beta g''(h_2)$$

The pressure gradient from Eqs. (2) and (25) is given by,

$$\frac{dp}{dx} = c_5(x) \quad (32)$$

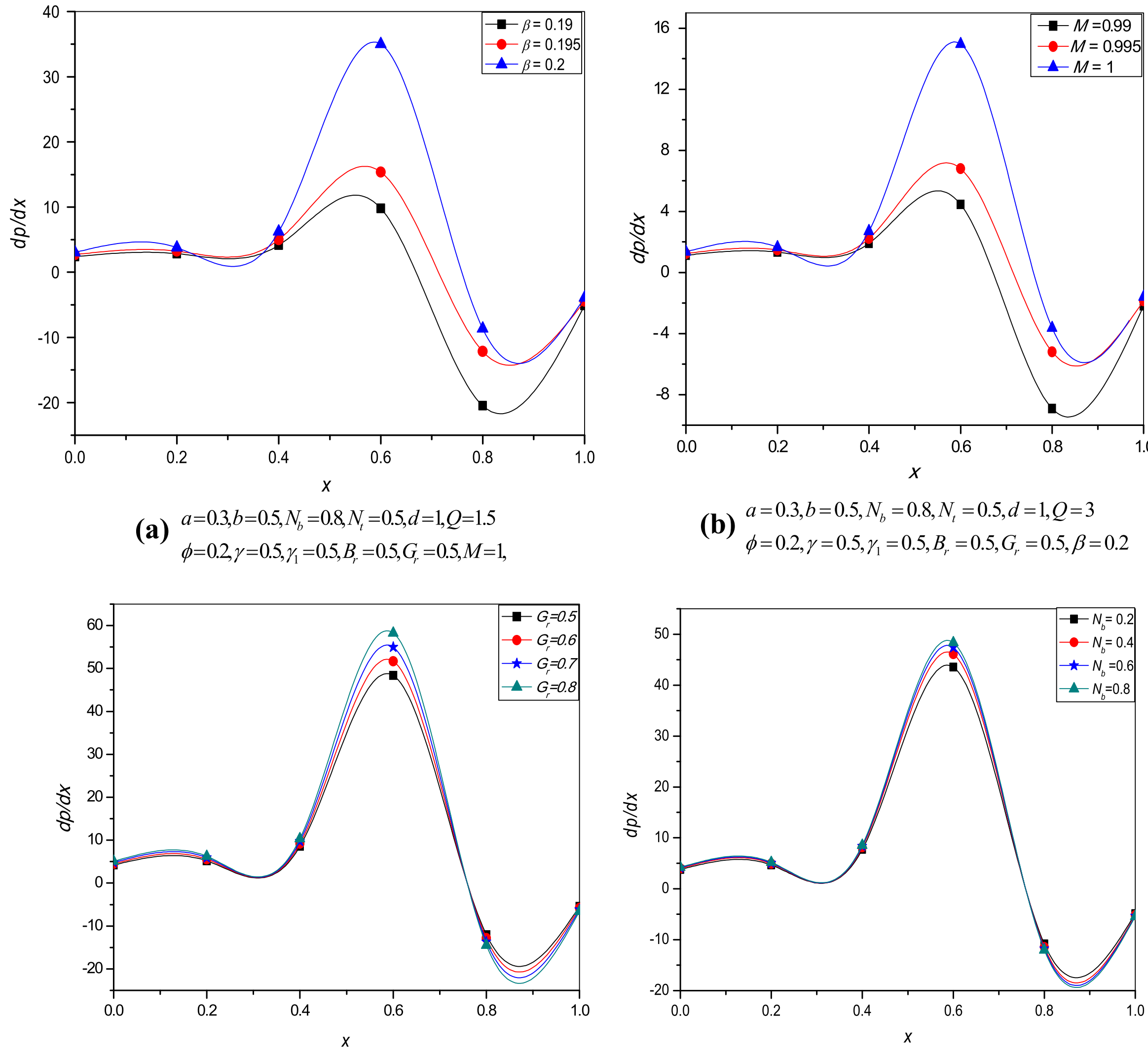

(a) $a=0.3, b=0.5, N_b=0.8, N_t=0.5, d=1, Q=1.5$
$\phi=0.2, \gamma=0.5, \gamma_1=0.5, B_r=0.5, G_r=0.5, M=1,$

(b) $a=0.3, b=0.5, N_b=0.8, N_t=0.5, d=1, Q=3$
$\phi=0.2, \gamma=0.5, \gamma_1=0.5, B_r=0.5, G_r=0.5, \beta=0.2$

(c) $a=0.3, b=0.5, N_b=0.8, N_t=0.5, d=1, Q=0.5$
$\phi=0.2, \gamma=0.5, \gamma_1=0.5, B_r=0.5, M=1, \beta=0.2$

(d) $a=0.3, b=0.5, G_r=0.5, N_t=0.5, d=1, Q=0.5$
$\phi=0.2, \gamma=0.5, \gamma_1=0.5, B_r=0.5, M=1, \beta=0.2$

Figure 11 Variation of the pressure gradient.

By solving linear system of Eq. (30) for constants,

$$c_5 = \frac{\left\{ \begin{array}{l} [(a_{11})(M^2 - M^4\beta^2)] + \left[s_1(a_{12})(M - M^2\beta)^2\right] \\ -\left[(R_1 - R_2)(a_{13})(M + M^2\beta)^3\right] + [(R_1 - R_2)e^{Mh_2}(M + M^2\beta)(M - M^2\beta] + \left[s_1(a_{14})(M + M^2\beta)^2\right] \end{array} \right\}}{\frac{1}{M^2}\left\{ \begin{array}{l} \left[2a_{15}(M + M^2\beta)^2\right] + [a_{16}(M^2 - M^4\beta^2)] \\ +\left[a_{17}(M - M^2\beta)^2\right] + \left[a_{18}(M + M^2\beta)(M - M^2\beta)^2\right] + \left[a_{19}(M + M^2\beta)^3\right] \end{array} \right\}} c_5 = \frac{a_{34}}{a_{35}}$$

$$c_7 = \frac{\left\{\frac{1}{M^2}[a_{20} - a_{21}][(a_{22})(a_{23}) - (a_{24})(a_{25})] - [(a_{26})(a_{23}) - (a_{27}(M + M^2\beta) - s_1 a_{14})a_{28}][a_{29}]\right\}}{\left\{[a_{30} - a_{31}]\frac{1}{M^2}[(a_{22})(a_{23}) - a_{32}(a_{33})]\right\}} c_7 = \frac{a_{36}}{a_{37}}$$

$$c_8 = \frac{a_{35}\left\{[(R_1 - R_2)a_{37} - (e^{-Mh_1} - e^{-Mh_2})a_{36}] - \left[\left(\frac{h_2 - h_1}{M^2}\right)(a_{34})(a_{37})\right]\right\}}{(a_{14})(a_{35})(a_{37})}$$

$$C_8 = \frac{a_{38}}{a_{39}}$$

$$C_6 = \frac{\{[(a_{35})(a_{37})][e^{Mh_1}(a_{35}) - (a_{34})]\} + \{[(a_{35})(a_{39})][a_{36} - R_1 M^2(a_{37})]\}}{(a_{35})(a_{37})(a_{39})}$$

The Pressure rise Δp in terms of the flow rate Q is given as

$$\Delta p = \int_0^1 \left(\frac{dp}{dx}\right)dx = \int_0^1 [c_5(x)]dx = \int_0^1 \left[\frac{\left\{\begin{array}{l}[(a_{11})(M^2 - M^4\beta^2)] + \left[s_1(a_{12})(M - M^2\beta)^2\right] \\ -\left[(R_1 - R_2)(a_{13})(M + M^2\beta)^3\right] + [(R_1 - R_2)e^{Mh_2}(M + M^2\beta)(M - M^2\beta] + \left[s_1(a_{14})(M + M^2\beta)^2\right]\end{array}\right\}}{\frac{1}{M^2}\left\{\begin{array}{l}\left[2a_{15}(M + M^2\beta)^2\right] + [a_{16}(M^2 - M^4\beta^2)] \\ +\left[a_{17}(M - M^2\beta)^2\right] + \left[a_{18}(M + M^2\beta)(M - M^2\beta)^2\right] + \left[a_{19}(M + M^2\beta)^3\right]\end{array}\right\}}\right]dx$$

$$= \int_0^1 \left[\frac{\left\{\begin{array}{l}[(a_{11})(M^2 - M^4\beta^2)] + \left[s_1(a_{12})(M - M^2\beta)^2\right] \\ -\left[(g(h_2) - g(h_1))(a_{13})(M + M^2\beta)^3\right] + [(g(h_2) - g(h_1))e^{Mh_2}(M + M^2\beta)(M - M^2\beta] + \\ \left[s_1(a_{14})(M + M^2\beta)^2\right]\end{array}\right\}}{\frac{1}{M^2}\left\{\begin{array}{l}\left[2a_{15}(M + M^2\beta)^2\right] + [a_{16}(M^2 - M^4\beta^2)] \\ +\left[a_{17}(M - M^2\beta)^2\right] + \left[a_{18}(M + M^2\beta)(M - M^2\beta)^2\right] + \left[a_{19}(M + M^2\beta)^3\right]\end{array}\right\}}\right]dx$$

$$+ \int_0^1 \left[\frac{(Q - 1 - d)\left[e^{Mh_2}(M + M^2\beta)(M - M^2\beta)^2 - (a_{13})(M + M^2\beta)^3\right]}{\frac{1}{M^2}\left\{\begin{array}{l}\left[2a_{15}(M + M^2\beta)^2\right] + [a_{16}(M^2 - M^4\beta^2)] \\ +\left[a_{17}(M - M^2\beta)^2\right] + \left[a_{18}(M + M^2\beta)(M - M^2\beta)^2\right] + \left[a_{19}(M + M^2\beta)^3\right]\end{array}\right\}}\right]dx \quad (33)$$

where $F = Q - 1 - d$.

4. Results and discussion

4.1. Pressure rise

The exact expression for the pressure rise is given by Eq. (33). It is observed that from Eq. (33) the pressure rise is always a decreasing function in terms of flow rate. The variation of pressure rise with flow rate for different values of slip parameter is presented in Fig. 2(a) and it is noticed that the pressure decreases with increasing slip parameter in the pumping region $-1 < Q < -3$ and converse behaviour occurs for the co pumping region $Q > -1$. The effect of increase in Hartmann number M on pressure rise is shown in Fig. 2(b). It is noticed that the pressure rise decreases with increasing Hartmann number M. From Fig. 2(c) it is observed that Δp decreases with increase in the values of thermophoresis parameter N_t. Fig. 2(d) reveals that the pressure rise increases with increase in N_b. Fig. 2(e) and (f) shows the increase in pressure rise when increase in local nanoparticle Grashof number B_r and local temperature Grashof number G_r. These behaviours are similar to Kothandapani and Prakash [32].

4.2. Temperature distribution

4.2.1. Temperature distribution (With slip parameters)

Variation of temperature profile θ for different values of thermophoresis parameter N_t and Brownian motion parameter N_b is plotted. It is observed that from Figs. 3 and 4 the temperature profile increases when thermophoresis parameter N_t and Brownian motion parameter N_b increase.

4.2.2. Temperature distribution (without slip parameter)

Variation of temperature profile θ for different values of thermophoresis parameter N_t and Brownian motion parameter N_b is plotted for $\gamma = \gamma_1 = 0$. The temperature distribution without thermal and concentration slip parameters is presented in Figs. 5 and 6. Comparing the results with previous Section 4.2.1, there are no remarkable differences observed for the effects of N_t and N_b.

4.3. Nanoparticle concentration

4.3.1. Nanoparticle concentration (with slip parameter)

Figs. 7 and 8 show the effects of thermophoresis parameter N_t and Brownian motion parameter N_b on the nanoparticle concentration σ. From Fig. 7 it is observed that σ decreases with increase in values of N_t and Fig. 8 shows the increase in σ as N_b increases and the results are similar to [26].

4.3.2. Nanoparticle concentration (without slip parameter)

The effects of thermophoresis parameter N_t and Brownian motion parameter N_b on the nanoparticle concentration σ are plotted for $\gamma = \gamma_1 = 0$. The nanoparticle concentration without thermal and concentration slip parameters is presented in Figs. 9 and 10. The results are similar as the Section 4.3.1.

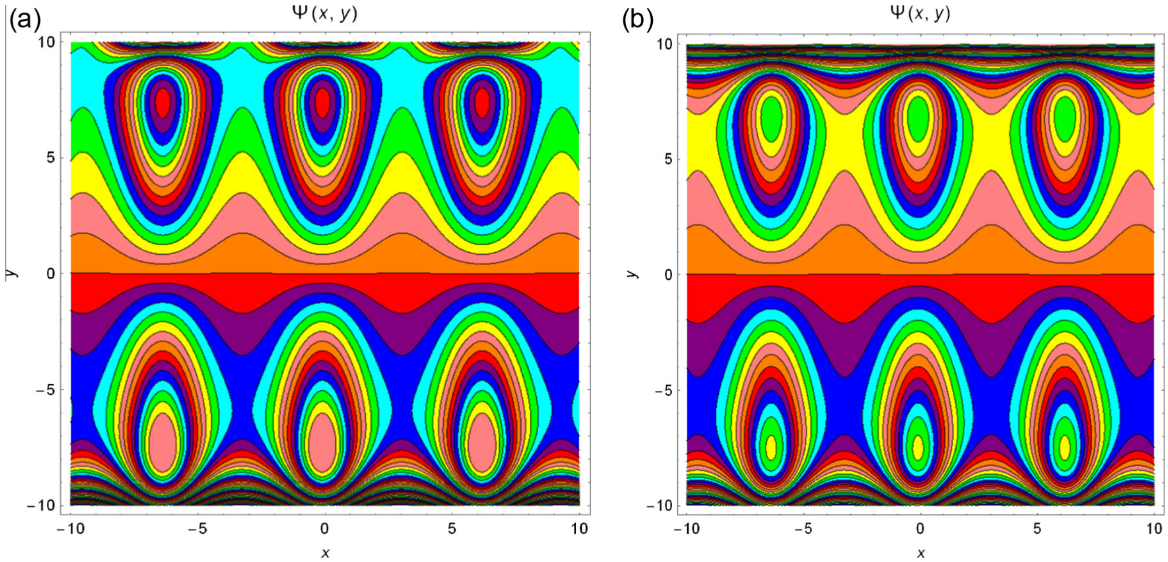

Figure 12 Streamlines for $a = 0.1,\ d = 1,\ b = 0.1,\ \phi = 0.2,\ \gamma = 0.5,\ \gamma_1 = 0.5,\ B_r = 2,\ M = 1,\ G_r = 0.5,\ N_b = 2,\ N_t = 2,\ \beta = 0.3$ and for different values of (a) $Q = 2.5$ and (b) $Q = 3$.

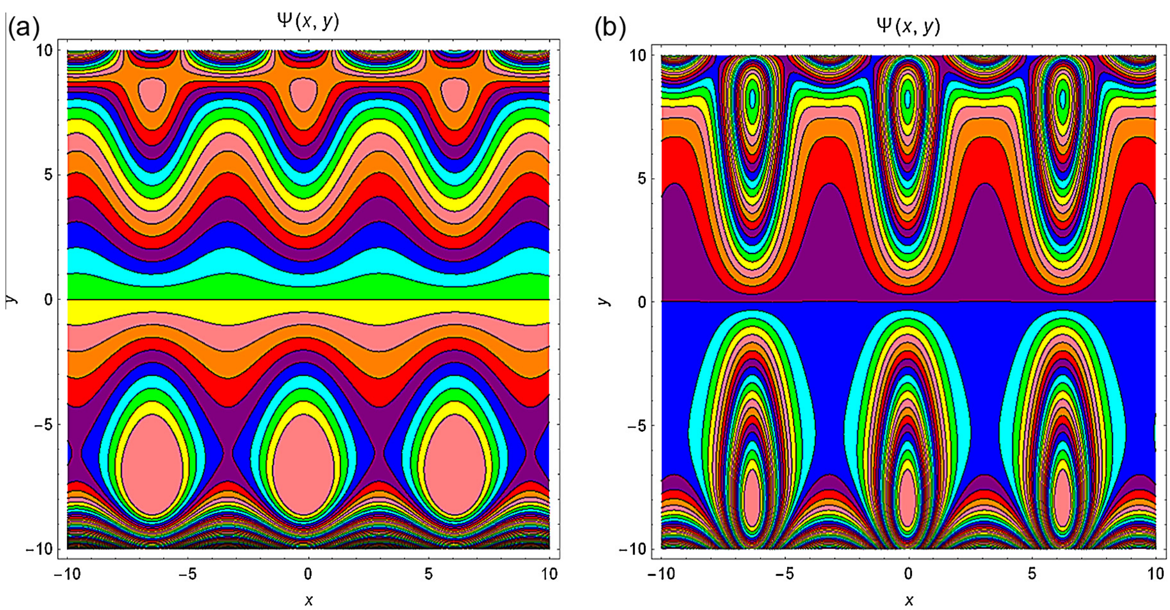

Figure 13 Streamlines for $Q = 2,\ d = 1,\ b = 0.1,\ \phi = 0.2,\ \gamma = 0.5,\ \gamma_1 = 0.5,\ B_r = 2,\ M = 1,\ G_r = 0.5,\ N_b = 2,\ N_t = 2,\ \beta = 0.3$ and for different values of (a) $a = 0$ and (b) $a = 0.3$.

4.4. Pressure gradient

Fig. 11(a)–(d) shows the variation of pressure gradient for different values of slip parameter, Hartmann number, Grashof number and thermophoresis parameters respectively. From these figures it is observed that the pressure gradient increases with increase in $\beta,\ M,\ G_r$ and N_b The small increase in $\beta,\ M$ effects the large differences in pressure gradient can be observed from Fig. 11(a) and (b) respectively and maximum pressure gradient occurs at $x = 0.6$ where it was $x = 0.45$ in [26].

4.5. Streamlines

The streamlines for different values of $Q,\ a,\ \beta$ and M are presented from Figs. 12–15. It is noticed from Fig. 12 that with increase in Q, the trapping bolus increases in the upper wall. Fig. 13 displays the influence of amplitude on both lower and upper walls, and the trapping bolus decreases with increasing amplitude. Fig. 14 reveals that the bolus increases at both walls of the channel when β increases and from Fig. 15 it is examined that the trapped bolus decreases as M increases at lower and upper walls.

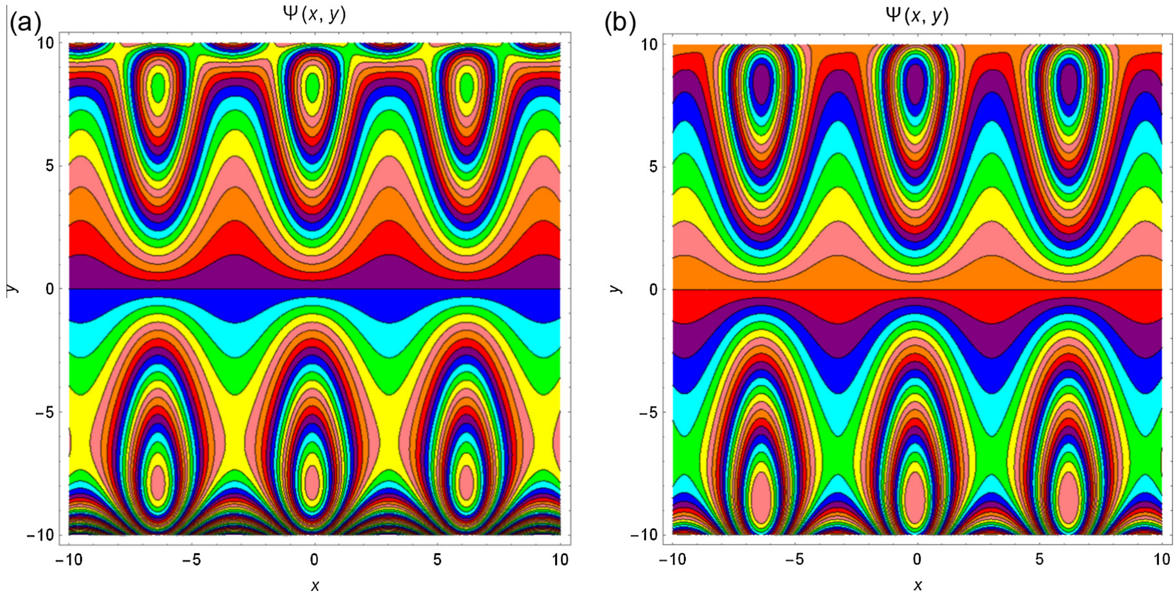

Figure 14 Streamlines for $a = 0.1,\ Q = 2,\ d = 1,\ b = 0.1,\ \phi = 0.2,\ \gamma = 0.5,\ \gamma_1 = 0.5,\ B_r = 2,\ M = 1,\ G_r = 0.5,\ N_b = 2,\ N_t = 2$ and for different values of (a) $\beta = 0.4$ and (b) $\beta = 0.6$.

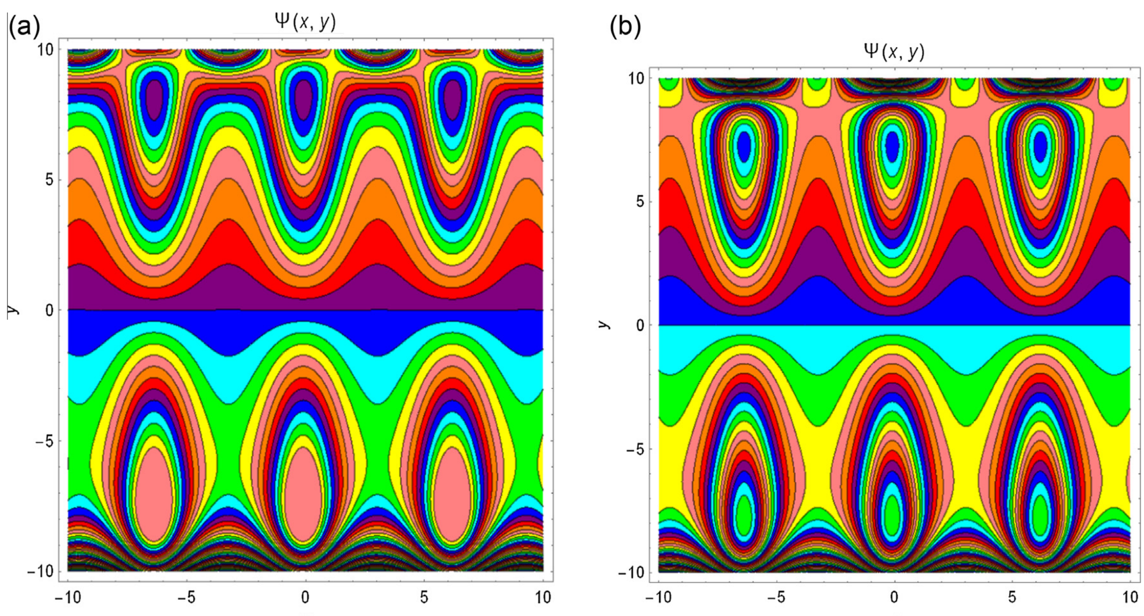

Figure 15 Streamlines for $a = 0.1,\ Q = 2,\ d = 1,\ b = 0.1,\ \phi = 0.2,\ \gamma = 0.5,\ \gamma_1 = 0.5,\ B_r = 2,\ G_r = 0.5,\ N_b = 2,\ N_t = 2,\ \beta = 0.3$ and for different values of (a) $M = 1$ and (b) $M = 1.1$.

5. Conclusions

The Peristaltic transport of conducting nanofluids under the effect of slip condition in an asymmetric channel is reported in the present work. The solution of the problem is solved exactly. Both slip effect and Magnetic effect on peristaltic transport of nanofluids are examined.

1. The pumping characteristics for different parameters are studied. The pressure rise decreases with increasing the parameters β, M, N_t and increases with increasing the parameters N_b, B_r, G_r respectively.
2. It is observed the large variations in pressure gradient by small increase in slip parameter and magnetic effects.
3. The temperature profile θ increases with increase in N_t and N_b and similar behaviour is observed without thermal and concentration slip parameters.
4. Nanoparticle concentration decreases with increasing N_t and increases with increasing N_b and the behaviour is the same when there are no thermal and concentration slip parameters.
5. It is observed that the pressure gradient increases with increasing parameters β, M, G_r and N_b'.
6. It is noticed that the size of the bolus increases with increasing parameters Q, β and decreases with increasing a, M respectively.

Acknowledgements

The authors thank the referees for their constructive comments which lead to betterment of the article.

Appendix A.

$$a_{11} = \left(s_1 e^{Mh_2} - 2s_2 e^{Mh_1} + s_2 e^{Mh_1} e^{2Mh_2}\right)$$

$$a_{12} = \left(e^{Mh_2} - e^{Mh_1} e^{2Mh_2} + \frac{e^{2Mh_2}}{e^{Mh_1}}\right)$$

$$a_{13} = \left(\frac{e^{2mh_1}}{2}\right)$$

$$a_{14} = (e^{Mh_1} - e^{Mh_2})$$

$$a_{15} = \left(e^{Mh_1} - \frac{e^{2Mh_1}}{e^{Mh_2}}\right)$$

$$a_{16} = \left(2e^{Mh_1} - e^{2Mh_1} e^{Mh_2} - e^{Mh_2}\right)$$

$$a_{17} = \left(e^{Mh_1} e^{2Mh_2} - \frac{e^{2Mh_2}}{e^{Mh_1}}\right)$$

$$a_{18} = e^{Mh_2}(h_2 - h_1)$$

$$a_{19} = (h_2 - h_1)\frac{e^{2Mh_1}}{e^{Mh_2}}$$

$$a_{20} = (R_1 - R_2)e^{Mh_1}(M + M^2\beta)$$
$$a_{21} = s_1(e^{Mh_1} - e^{Mh_2})$$
$$a_{22} = (e^{Mh_1})(M + M^2\beta) - (e^{Mh_2})(M - M^2\beta)$$
$$a_{23} = \left(1 - \tfrac{e^{Mh_1}}{e^{Mh_2}}\right)(M + M^2\beta) + \left(1 - \tfrac{e^{Mh_2}}{e^{Mh_1}}\right)(M - M^2\beta)$$
$$a_{24} = (h_2 - h_1)e^{Mh_1}(M + M^2\beta) + (e^{Mh_1} - e^{Mh_2})$$
$$a_{25} = \left(\tfrac{e^{Mh_1}}{e^{Mh_2}}(M + M^2\beta)^2 - \tfrac{e^{Mh_2}}{e^{Mh_1}}(M - M^2\beta)^2\right)$$
$$a_{26} = \left(s_1 e^{Mh_1}(M - M^2\beta) - s_2 e^{Mh_1}(M + M^2\beta)\right)$$
$$a_{27} = (R_1 - R_2)e^{Mh_1}$$
$$a_{28} = \left(\tfrac{e^{Mh_1}}{e^{Mh_2}}(M + M^2\beta)^2 - \tfrac{e^{Mh_2}}{e^{Mh_1}}(M - M^2\beta)\right)$$

$$a_{29} = \left[\left(\tfrac{h_2 - h_1}{M^2}\right)e^{Mh_1}(M + M^2\beta) + \tfrac{1}{M^2}(e^{Mh_1} - e^{Mh_2})\right]$$
$$a_{30} = e^{Mh_1}(e^{-Mh_1} - e^{-Mh_2})(M + M^2\beta)$$
$$a_{31} = e^{-Mh_1}(e^{Mh_1} - e^{Mh_2})(-M + M^2\beta)$$

$$a_{32} = \left((h_2 - h_1)e^{Mh_1}(M + M^2\beta) + (e^{Mh_1} - e^{Mh_2})\right)$$
$$a_{33} = \left(\tfrac{e^{Mh_1}}{e^{Mh_2}}(M + M^2\beta)^2 - \tfrac{e^{Mh_2}}{e^{Mh_1}}(M - M^2\beta)^2\right)$$

$$a_{34} = \left\{\begin{array}{l} \left[(a_{11})(M^2 - M^4\beta^2)\right] + \left[s_1(a_{12})(M - M^2\beta)^2\right] \\ -\left[(R_1 - R_2)(a_{13})(M + M^2\beta)^3\right] \\ +\left[(R_1 - R_2)e^{Mh_2}(M + M^2\beta)(M - M^2\beta\right] \\ +\left[s_1(a_{14})(M + M^2\beta)^2\right] \end{array}\right\}$$

$$a_{35} = \frac{1}{M^2}\left\{\begin{array}{l} \left[2a_{15}(M + M^2\beta)^2\right] + \left[a_{16}(M^2 - M^4\beta^2)\right] \\ +\left[a_{17}(M - M^2\beta)^2\right] \\ +\left[a_{18}(M + M^2\beta)(M - M^2\beta)^2\right] \\ +\left[a_{19}(M + M^2\beta)^3\right] \end{array}\right\}$$

$$a_{36} = \left\{\frac{1}{M^2}[a_{20} - a_{21}][(a_{22})(a_{23}) - (a_{24})(a_{25})] - [(a_{26})(a_{23}) - (a_{27}(M + M^2\beta) - s_1 a_{14})a_{28}][a_{29}]\right\}$$

$$a_{37} = \left\{[a_{30} - a_{31}]\frac{1}{M^2}[(a_{22})(a_{23}) - a_{32}(a_{33})]\right\}$$

$$a_{38} = a_{35}\left\{\left[(R_1 - R_2)a_{37} - (e^{-Mh_1} - e^{-Mh_2})a_{36}\right] - \left[\left(\frac{h_2 - h_1}{M^2}\right)(a_{34})(a_{37})\right]\right\}$$

$$a_{39} = (a_{14})(a_{35})(a_{37})$$

References

[1] T.W. Latham, Fluid Motion in a Peristaltic Pump M.Sc. Thesis, Massachusetts Institute of Technology, Cambridge, 1966.

[2] A.H. Shapiro, M.Y. Jaffrin, S.L. Weinberg, Peristaltic pumping with long Wavelengths and low Reynolds number, J. Fluid Mech. 37 (1969) 799–825.

[3] T.F. Zien, S.A. Ostrach, A long wave approximation to Peristaltic motion, J. Biomech. 3 (1970) 63–75.

[4] L.M. Srivastava, V.P. Srivastava, S.N. Sinha, Peristaltic transport of a physiological fluid: PartI: Flow in non-uniform geometry, Biorheology 20 (1983) 153–166.

[5] R.A. Ramachandra, S. Usha, Peristaltic transport of two immiscible viscous fluids in a circular tube, J. Fluid Mech. 298 (1995) 271–285.

[6] K. Vajravelu, S. Sreenadh, V.R. Babu, Peristaltic transport of Herschel–Bulkley fluid in an inclined tube, Int. J. Non-Linear Mech. 40 (2005) 83–90.

[7] K. Vajravelu, S. Sreenadh, P. Lakshminarayana, The influence of heat transfer on Peristaltic transport of Jeffrey fluid in a vertical porous stratum, Commun. Nonlinear Sci. Numer. Simul. 16 (2011) 3107–3125.

[8] K. Vajravelu, S. Sreenadh, K. Rajinikanth, Changhoon Lee, Peristaltic transport of a Williamson fluid in asymmetric channel with permeable walls, Nonlinear Anal. Real World Appl. 13 (2012) 2804–2822.

[9] S.U.S. Choi, Jeffrey A. Eastman, Enhancing Thermal Conductivity of Fluids with Nanoparticles, ASME Publications, 1995.

[10] S.U.S. Choi, Z.G. Zhang, W. Yu, F.E. Lockwood, E.A. Grulke, Anomalous thermal conductivity enhancement in nanotubes suspensions, Appl. Phys. Lett. 79 (2001) 2252–2254.

[11] J. Buongiorno, Connective transport in nanofluids, ASME, J. Heat Transfer 128 (2005) 240–250.

[12] K.S. Mekheimer, Y. Abd elmaboud, The influence of heat transfer and magnetic field on Peristaltic transport of Newtonian fluid in a vertical annulus: application of an endoscope, Phys. Lett. A 372 (2008) 1657–1665.

[13] S. Srinivas, R. Gayathri, M. Kothandapani, The influence of slip conditions, wall properties and heat transfer and on MHD peristaltic transport, Comput. Phys. Commun. 180 (2009) 2115–2122.

[14] S. Srinivas, R. Muthuraj, Peristaltic transport of a Jeffrey fluid under the effect of slip in an inclined asymmetric, Int. J. Appl. Mech. 2 (2) (2010) 437–455.
[15] N.S. Akbar, S. Nadeem, Endoscopic effects on peristaltic flow of a nanofluid, Commun. Theor. Phys. 56 (2011) 761–768.
[16] A.V. Ramana Kumari, G. Radhakrishnamacharya, Effect of slip on heat transfer to Peristaltic transport in the presence of magnetic field with wall effects, ARPN J. Eng. Appl. Sci. 6 (7) (2011) 119–131.
[17] N.S. Akbar, S. Nadeem, T. Hayat, A.A. Hendi, Peristaltic transport of a nanofluid in non-uniform tube, Heat Mass Transfer 48 (2012) 451–459.
[18] N.S. Akbar, S. Nadeem, Peristaltic flow of a Phan-Thien–Tanner nanofluid in a diverging tube, Heat Transfer 41 (2012) 10–22.
[19] M. Mustafa, S. Hina, T. Hayat, A. Alsaedi, Influence of wall properties on the Peristaltic flow of a nanofluid: analytic and numerical solutions, Int. J. Heat Mass Transfer 55 (2012) 4871–4877.
[20] N.S. Akbar, S. Nadeem, T. Hayat, A.A. Hendi, Peristaltic transport of a nanofluid with slip Effects, Maccanica 47 (2012) 1283–1294.
[21] S. Srinivas, R. Muthuraj, J. Sakina, A note on the influence of heat and mass transfer on a Peristaltic flow of a viscous fluid in a vertical asymmetric channel with wall slip, Chem. Ind. Chem. Eng. Quart. 18 (3) (2012) 483–493.
[22] S. Akram, S. Nadeem, A. Ghafoor, C. Lee, consequences of nanofluid on Peristaltic flow in an asymmetric Channel, Int. J. Basic Appl. Sci. 12 (2013) 75–96.
[23] N.S. Akbar, S. Nadeem, Changhoon Lee, Zafar Hayat Khan, Rizwan UI Haq, Numerical study of Williamson nanofluid in an asymmetric channel, Results Phys. 3 (2013) 161–166.
[24] A. Ebaid, E.H. Aly, Exact Analytical Solution of the Peristaltic Nanofluids Flow in an Asymmetric Channel with Flexible Walls and Slip Condition: Application to Cancer Treatment, Hindawi Publishing Corporation, 2013.
[25] M. Mustafa, S. Hina, T. Hayat, A. Alsaedi, Slip effects on the Peristaltic motion of nano fluid in a channel with wall properties, ASME J. Heat Transfer 135 (2013).
[26] E.H. Aly, A. Ebaid, Exact analytical solution for the peristaltic flow of nanofluids in an asymmetric channel with slip effect of the velocity, temperature and concentration, J. Mech. 30 (2014) 411–422.
[27] S. Akram, S. Nadeem, Consequence of nanofluid on peristaltic transport of a hyperbolic Tangent fluid model in the occurrence of apt (tending) magnetic field, J. Magnet. Magnet. Mater. 358 (2014) 183–191.
[28] M. Mustafa, S. Hina, T. Hayat, B. Ahmad, Influence of induced magnetic field on the Peristaltic flow of nanofluid, Maccanica 49 (2014) 521–534.
[29] S. Hina, M. Mustafa, S. Abbasbandy, T. Hayat, A. Alsaedi, Peristaltic motion of nanofluid in a curved channel, J. Heat Transfer ASME 136 (2014).
[30] Obaid Ullah Mehmood, Norzieha Mustapha, Sharidan Shafie, T. Hayat, Partial slip effect on heat and mass transfer of MHD peristaltic transport in a porous medium, Sains Malaysiana 43 (7) (2014) 1109–1118.
[31] Tasawar Hayat, Fahad Munir Abbasi, Bashir Ahmadz, Ahmed Alsaedi, Peristaltic transport of Carreau-Yasuda fluid in a curved channel with slip effects, Plos One 9 (4) (2014), e95070.
[32] M. Kothandapani, J. Prakash, Effect of radiation and magnetic field on peristaltic transport of nanofluids through a porus space in a tapered asymmetric channel, J. Magnet. Magnet. Mater. 378 (2015) 152–163.
[33] M. Kothandapani, J. Prakash, The peristaltic transport of Carreau nanofluid under effect of a magnetic field in a tapered asymmetric channel: application to cancer therapy, J. Mech. Med. Biol. 15 (2015) 1550030–1550062.
[34] M. Kothandapani, J. Prakash, Effects of thermal radiation parameter and magnetic field on the peristaltic motion of Williamson nanofluids in a tapered asymmetric channel, Int. J. Heat Mass Transfer 51 (2015) 234–245.
[35] K. Nirmala, R. Muthuraj, S. Srinivas, D. Lourdu Immaculate, Combined effects of hall current, wall slip, viscous dissipation and soret effect on MHD Jeffrey fluid flow in a vertical channel with Peristalsis, JP J. Heat Mass Transfer 12 (2) (2015) 131–165.